

Micro-pixel Image Position Sensing Testbed

Bijan Nemati*, Michael Shao, Chengxing Zhai, Hernan Erlic, Xu Wang, Renaud Goullioud

Jet Propulsion Laboratory, California Institute of Technology
4800 Oak Grove Drive, Pasadena, CA, U.S.A. 91109

ABSTRACT

The search for Earth-mass planets in the habitable zones of nearby Sun-like stars is an important goal of astrophysics. This search is not feasible with the current slate of astronomical instruments. We propose a new concept for micro-arcsecond astrometry which uses a simplified instrument and hence promises to be low cost. The concept employs a telescope with only a primary, laser metrology applied to the focal plane array, and new algorithms for measuring image position and displacement on the focal plane. The required level of accuracy in both the metrology and image position sensing is at a few micro-pixels. We have begun a detailed investigation of the feasibility of our approach using simulations and a micro-pixel image position sensing testbed called MCT. So far we have been able to demonstrate that the pixel-to-pixel distances in a focal plane can be measured with a precision of 20 micro-pixels and image-to-image distances with a precision of 30 micro-pixels. We have also shown using simulations that our image position algorithm can achieve accuracy of 4 micro-pixels in the presence of $\lambda/20$ wavefront errors.

Keywords: Astrometry, Exoplanets, CCD, Metrology, Micro-pixel

1. INTRODUCTION

The discovery of the first extra-solar planet in 1995 ushered in a new era in this important segment of astrophysics.¹ The interest in exoplanets stems not only from their importance to understanding the mechanisms effective in the formation of stellar systems, but also from the philosophically profound question of whether the Earth represents a rare position as a life-bearing planet. The initial expectation that Earths should be ubiquitous have been met with observations surprisingly pointing in the opposite direction. For example, the latest data from the Kepler mission indicates that the fraction of stars hosting an Earth-mass planets in their habitable zone, η_{Earth} , is only 3 percent.² These findings point to the importance of detailed studies of nearby stars for Earth-like planets in their habitable zones, since it is with these systems that the most detailed studies such as imaging and spectroscopy is more easily achievable.

Among the current group of active exoplanet missions, none possesses the sensitivity to Earth-mass planets in the habitable zones of nearby stars at an adequate level to ensure detection. The Space Interferometry Mission (SIM) was a mission capable of such a detection, but was cancelled last year after receiving a low ranking from the 2010 Decadal Survey of Astronomy and Astrophysics. SIM, however, may have provided the seeds for a new type of mission that may be able to reach this challenging sector of the exoplanet phase space. With use of high-precision metrology developed in the SIM program, along with new image position sensing methodology, we have arrived at a novel approach to detect nearby Earths using a relatively modest space-based astrometric instrument.

The new approach, exemplified in the NEAT concept proposed this year to ESA, uses a ‘staring’ telescope with a single, 1 meter-class mirror and a long (20-40 m) focal length to image a candidate host star against a background of other stars that serve as astrometric references.³ A per-epoch error of 1 μ s would be adequate, after 200 observations spanning five years, to achieve the sensitivity to detect an Earth at a distance of 10 parsecs.^{4,5} The use of a single-mirror telescope is necessitated by the otherwise prohibitive beamwalk errors that would arise for objects located in different parts of the field of view. The footprints of stars in different parts of the field would be identical on the primary but would be different on a secondary and/or tertiary mirror if these were part of the telescope design. The difference in the footprints,

* bijan.nemati@jpl.nasa.gov; phone 1 (818) 354-0883

© 2011 California Institute of Technology. Government sponsorship acknowledged.

coupled with even microscopic changes in the wavefront error of secondary or tertiary mirrors over the course of a multi-year mission, would create large astrometric errors. The simple architecture proposed here would alleviate this problem, but was never considered seriously for this application until now, because of the additional obstacles posed by another source of error: focal plane systematics. Normally one assumes that the pixels in the focal plane are on a regular grid of known spacing, and that the quantum efficiency within each pixel is flat. At this level of precision, however, neither assumption is adequate: the intra-pixel quantum efficiencies are not flat and the pixel locations are not regular. Moreover, the focal plane array can distort and change with thermal variations. These previously daunting problems are now solved through the use of metrology: we can measure the distance between stellar images in the focal plane using laser fringes as a highly stable yardstick. The focal plane array itself now becomes merely an intermediary. The laser fringes will not only tell us where each pixel is, but what the pixel response function looks like for photons arriving anywhere within or near the pixel.

Putting all this together, the concept incorporates three key features: 1) a single-mirror, long-focus telescope to reduce beamwalk errors; 2) laser metrology fringes scanning the focal plane in order to calibrate the pixel locations and the intra-pixel quantum efficiency (QE) variations, and 3) low-bias image position reconstruction algorithm.

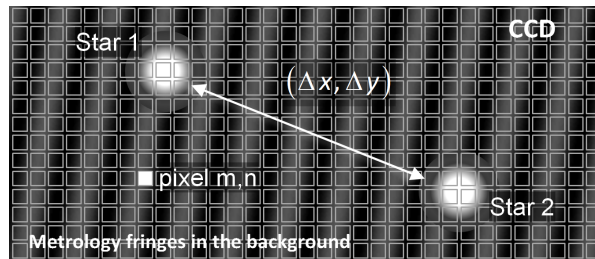


Figure 1: A new approach in staring astrometry: measure the distance between the stars using laser fringes as a highly stable yardstick, with the CCD as an intermediary. Here a single CCD frame is shown with two stars: the distance maps directly to astrometric angle. The metrology fringes to calibrate each pixel’s location and intra-pixel QE map.

This concept is described in Figure 2. Fibers with tips fixed to the primary mirror illuminate the focal plane with laser light. Laser light is injected to one pair of fibers at a time, with a small frequency offset (typically a few Hz) between the two fibers. This produces parallel fringes that move across the focal plane. Each pixel sees a sinusoidal light intensity variation. The phase of the sine wave observed by any pixel in the focal plane, compared to that measured by some reference pixel, gives the relative position of the given pixel in the direction parallel to the motion of the fringes. To get a two-dimensional position, a different pair of fibers is turned on next. In the same way, the position of every given pixel is measured relative to the reference pixel along this new direction of moving fringes. As we will describe in more detail in below, this process provides not only the positions but also the intra-pixel quantum efficiencies for all the pixels at the micro-pixel level. This improves the state of the art in this area by about two orders of magnitude.⁶

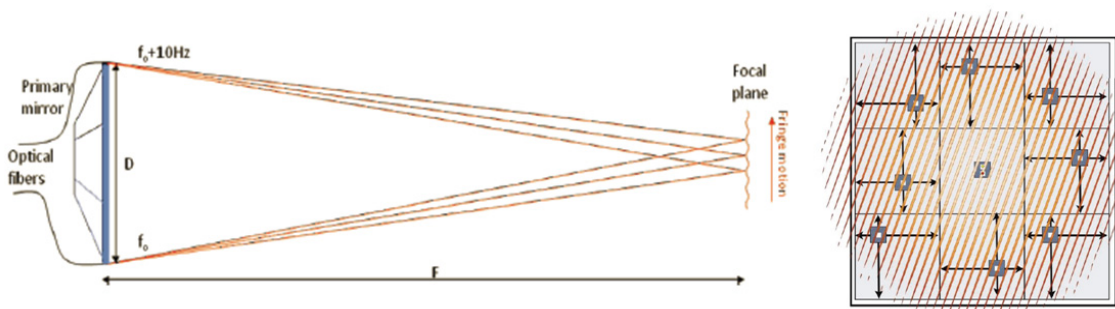


Figure 2: The Nearby Earth Astrometric Telescope concept is based on our staring astrometry approach.

High-precision centroiding will require that a star image be at least Nyquist sampled by the focal plane array, that is, the star spot should span at least two pixels (Figure 1). The size of a stellar image on the focal plane is approximately equal to $f\lambda/D$, where f is the focal length, D is the primary mirror diameter, and λ is the mean wavelength of the starlight. For

a 1 meter telescope with a 20 m focal length looking at a star with a mean wavelength of 640 nm, Nyquist-sampling the star requires that each pixel correspond to 66 mas (milli arcsecond) on the sky. For such a telescope, then, 1 μ as accuracy on the sky corresponds to 15 μ pix accuracy on the CCD.

Figure 3 shows a simplified top-level error budget for our concept mission. Holding some reserve, we target a performance of 0.9 μ as in differential measurement accuracy (DMA), which is the metrology-calibrated distance between stellar images in the focal plane. This error is then sub-allocated to the main error categories. The boxes that are important from a technology demonstration standpoint include the precision in measuring the star locations (shaded green), the precision in the metrology measurements (shaded purple) and the accuracy of combining the starlight and metrology (shaded pink). Also indicated in the figure are the main tests that need to be conducted in order to demonstrate this technology. The inter-star differential measurement precision (DMP) test ascertains that the photon noise and random vibration noise are low enough to allow a star-star measurement with 10 μ pix precision. The metrology DMP test demonstrates that the metrology approach can find the pixel locations with the precision required (6 μ pix allowed in this case). The most challenging test is the calibrated differential measurement accuracy (DMA) demonstration, which shows that the measured inter-star distances, after being corrected for focal plane motion and deformation, are repeatable to 13 μ pix.

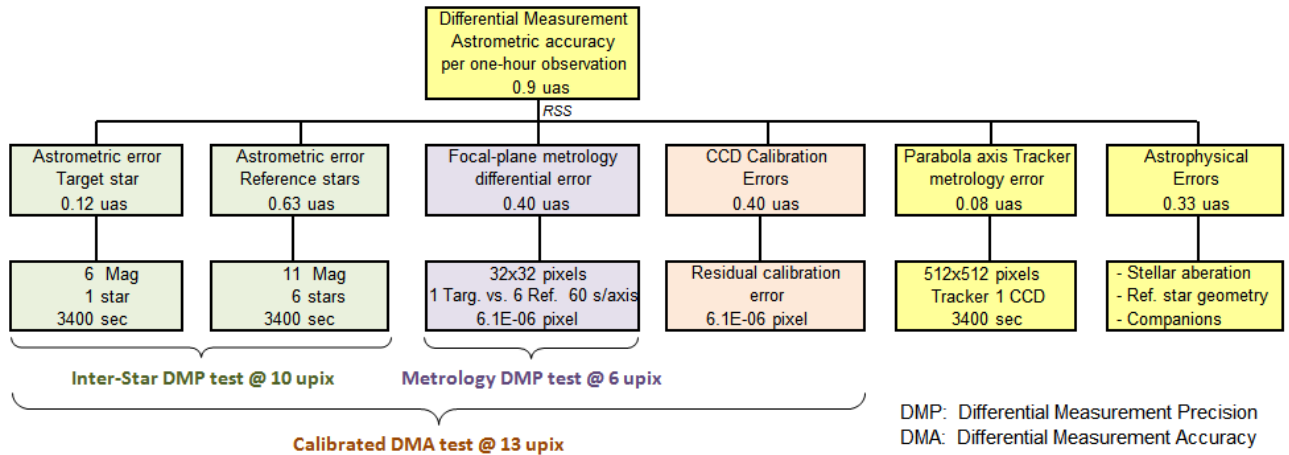


Figure 3: A simplified top-level error budget showing the three types of initial demonstration tests.

The Micro-pixel Centroiding Testbed (MCT) was a small breadboard testbed built to get an initial assessment of the feasibility of this error budget. The testbed was in operation in the last quarter of the 2010 calendar year. In this paper we give an overview of the algorithm and then move on to describe the testbed, the results so far, and what future work we are planning to do.

2. MICRO-PIXEL IMAGE ESTIMATION

For micro-pixel level of precision, the focal plane brightness centroid is an adequate measure of the position of a stellar image. A focal plane array, such as a CCD, samples the focal plane brightness distribution at the scale of pixels, which are neither precisely located on a regular grid nor have uniform quantum efficiency. As a result, the simple centroid formula that assigns each pixel a single, flat weight will incur large systematic errors. Fitting the point spread function (PSF) to estimate centroid position has been popularly used for achieving high-precision centroid estimation.⁷ The accuracy crucially depends on the knowledge of the PSF. A typical choice is a Gaussian template function, which is not sufficient for micro-pixel level accuracy. In our approach we attempt to arrive at an estimate the actual PSF.

Using the principles of Fourier optics, the PSF is given by the Fourier transform of the electric field at the telescope input pupil. Because any real instrument's collecting aperture has a finite size, the signal at the focal plane is bandwidth limited. The highest spatial frequency of the focal plane image is $D / \lambda f$, where D is the diameter of the telescope, λ is the wavelength, and f is the focal length. This enables us to reconstruct the PSF with high fidelity from a pixilated image, relying on the sampling theorem. Accordingly, we require that the CCD pixels to be small enough that the images are *at least* Nyquist sampled. In terms of the telescope parameters, this means the pixel size should be less than $\lambda f / (2D)$ or

alternatively $\lambda F\# / 2$. If the mean stellar wavelength is 600 nm and the telescope $F\#$ is 40 (such as in the NEAT concept), this corresponds to a maximum pixel size of 12 μm . For exoplanet detection, we only need to measure *temporal variations* of star positions, therefore it is sufficient to estimate the displacement between two images of the same star. We use one of the two images to reconstruct the PSF and then resample it at different locations. The location at which the resampled image best matches the second image is the estimation of the displacement between the two images.

Figure 4 summarizes our approach. We use laser metrology to characterize the detector pixel response functions in Fourier space. With this, we reconstruct a point spread function using a pixilated image. The PSF is then resampled at a relative location of $(\Delta x_c, \Delta y_c)$ from the original position and compared with the second image. The location $(\Delta x_c, \Delta y_c)$ at which the resampled PSF best matches the second image is taken as the estimated displacement of the second image from the first image.

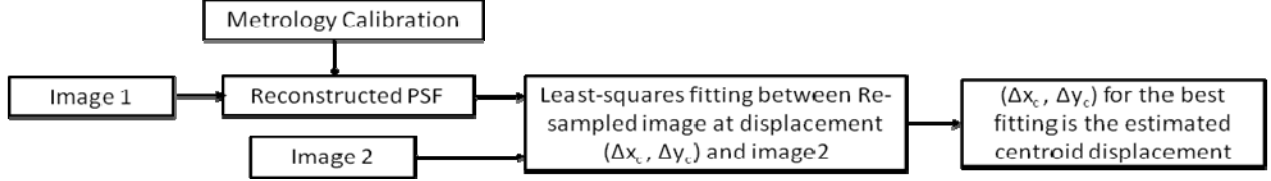


Figure 4: Our approach uses calibration and Fourier interpolation to greatly enhance image centroiding accuracy. Calibrating the focal plane pixel response function in this way has the potential to dramatically expand the capabilities of observational instruments in astronomy.

If the pixels were regular with an ideal, top-hat response, the only systematic error in this approach would be from the finite size of the CCD window chosen around the PSF. Based on simulations, we find that this truncation error can be kept under 1 μpix if we use a 32x32 pixel window that spans out to about the 7th Airy ring. However, the pixel response of the CCD is not flat, due to quantum efficiency (QE) variations within each pixel and the diffusion of photo-electrons between pixels. We can address these complications by defining a pixel response function $R_{mn}(x, y)$ which gives the response of pixel (m, n) , in photo-electrons recorded, to a point illumination (i.e. a delta function) at location (x, y) anywhere in the focal plane. For a general illumination pattern $I(x, y)$, the pixel output is a convolution of the pixel response function:

$$I_{mn} = \iint dx dy R_{mn}(x, y) I(x, y) \quad (1)$$

Note that the pixel response function conveniently captures 1) the overall location of the pixel, 2) the variation of the QE within a pixel, and 3) the photo-electron diffusion between pixels.

If all the pixels have the same response function, the pixilated image still corresponds to samples of a bandwidth limited function because the effect of the convolution is simply a multiplicative factor to the spectrum and thus does not affect the bandwidth. Measurements of actual detector characterization measurements show that, for a typical CCD, the pixel response functions of all the pixels do share a dominant common portion.⁸ A small pixel-to-pixel variation does exist which is significant in micro-pixel centroiding. This calls for accurate detector response calibration.

It is convenient to calibrate the pixel response function in Fourier space because of the limited bandwidth in the signal. This can be achieved by illuminating the detector with a sinusoidal pattern, of the form:

$$I(x, y) = I_0 + A \cos(k_x x + k_y y + \varphi). \quad (2)$$

The counts at pixel (m, n) are then related to the Fourier transform of the pixel response function via

$$I_{mn} = I_0 \tilde{R}_{mn}(0, 0) + A \operatorname{Re} \left[\tilde{R}_{mn}(k_x, k_y) e^{i\varphi} \right] \quad (3)$$

$$\tilde{R}_{mn}(k_x, k_y) \equiv \iint dx dy e^{i(k_x x + k_y y)} R_{mn}(x, y) \quad (4)$$

We generate the cosine intensity pattern by interfering two metrology laser beams, from the ends of two fibers mechanically fixed to the primary mirror of the astrometric telescope. We apply a frequency offset between the laser metrology beams so that the spatial fringes move across the focal plane as the applied phase difference $\varphi = 2\pi \Delta f t$ grows linearly with time. The temporal variation of I_{mn} is a sinusoidal function whose amplitude and phase allow us to estimate $\tilde{R}_{mn}(k_x, k_y)$. We can expand this function as a power series:

$$\begin{aligned} \tilde{R}_{mn}(k_x, k_y) = & \tilde{R}_{mn}(0, 0) \cdot \exp\left\{i\left[k_x(x_{mn} + \Delta x_{mn}) + k_y(y_{mn} + \Delta y_{mn})\right]\right\} \\ & \times \left[1 + \alpha_{mn}k_x^2 + \beta_{mn}k_y^2 + \gamma_{mn}k_xk_y + \dots\right] \end{aligned} \quad (5)$$

where $\tilde{R}_{mn}(0, 0)$ is the flat field response, and $(\Delta x_{mn}, \Delta y_{mn})$ represents an effective pixel location deviation from a regular grid (x_{mn}, y_{mn}) . In the square bracket are the higher order terms. By measuring $\tilde{R}_{mn}(k_x, k_y)$ at different spatial frequencies, we can estimate the parameters in Equation (5). Using a numerical simulation that assumes 5% rms QE fluctuations within a pixel, we find that it is sufficient to keep terms up to the third power of the wave number for achieving 5 μpix accuracy.⁹

We also investigated systematic errors in our centroid displacement estimation algorithm using simulated image pairs and simulated pixel metrology calibration errors. We repeated the estimation for simulated various centroid displacements along both x (row) and y (column) directions. Figure 5 displays the results. We found that the RMS estimation error over the +/- 0.5 pix centroid displacement range is less than 4 μpix , with the error being small near the center (smallest displacements) and increasing towards the edges.

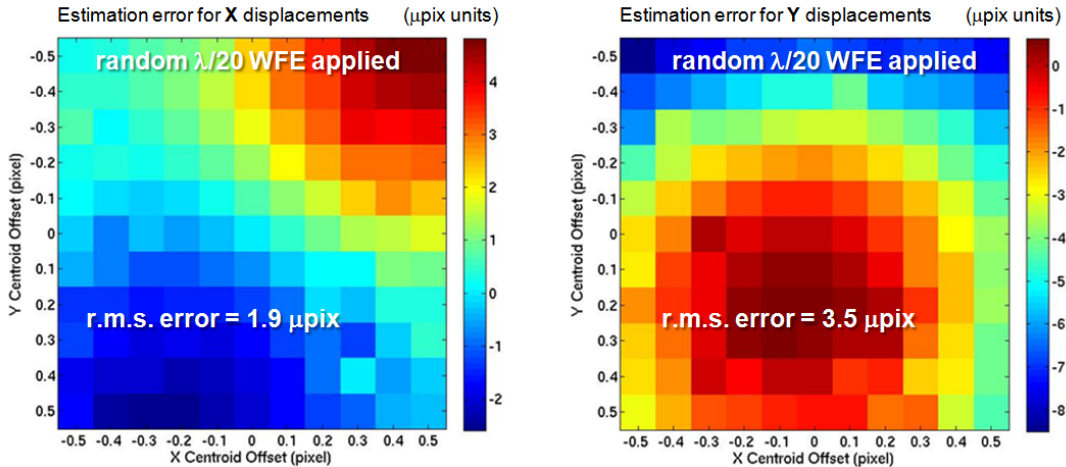


Figure 5: Simulation results showing the expected systematic errors in our estimation of image displacements for various applied x and y displacements. A wavefront error of $\lambda/20$ was simulated. The grids correspond to relative two-dimensional centroid displacements along x and y within the range $[-0.5, 0.5]$ pix. The error is expressed in μpix units.

3. THE MCT TESTBED

The Micro-pixel Centroiding Testbed (MCT) was a small breadboard built mostly out of SIM spare parts prior to its shutdown. Figure 6 below highlights some of the most important features of the MCT configuration.

The testbed was located within the 40-foot long SIM vacuum chamber, though it occupied only a small part at one end. The detector for the test was a back-illuminated, E2V CCD39 with an 80 x 80 array of 24 μm pixels. The CCD was illuminated with metrology fringes and stars as needed for different aspects of the test. The middle image on the top row of Figure 6 shows a single frame taken with the detector, showing simultaneously some metrology fringes and three stars. In the top right of Figure 6, we see the optical bench. This was originally a spare SIM beam launcher component –

a ULE bench with a collimator parabola glued to it. The parabola was masked to allow a 14 mm ‘primary’ mirror to be defined. A bundle consisting of 7 closely packed fibers was mounted with a defocus in such a way to create an image at an effective focal length of 1.1 m and an F# of about 80. The middle image, top row, shows three of the seven stars created this way. The sampling of the PSF’s, defined as the number of pixels per $\lambda f / D$, was 2.55. Later on in the experiment, the aperture diameter was reduced to allow better sampling. Also mounted on the ULE block was a low expansion ‘metrology block’, on which was mounted six metrology fibers with their tips pointed at the detector. These would be illuminated pairwise to create various fringes.

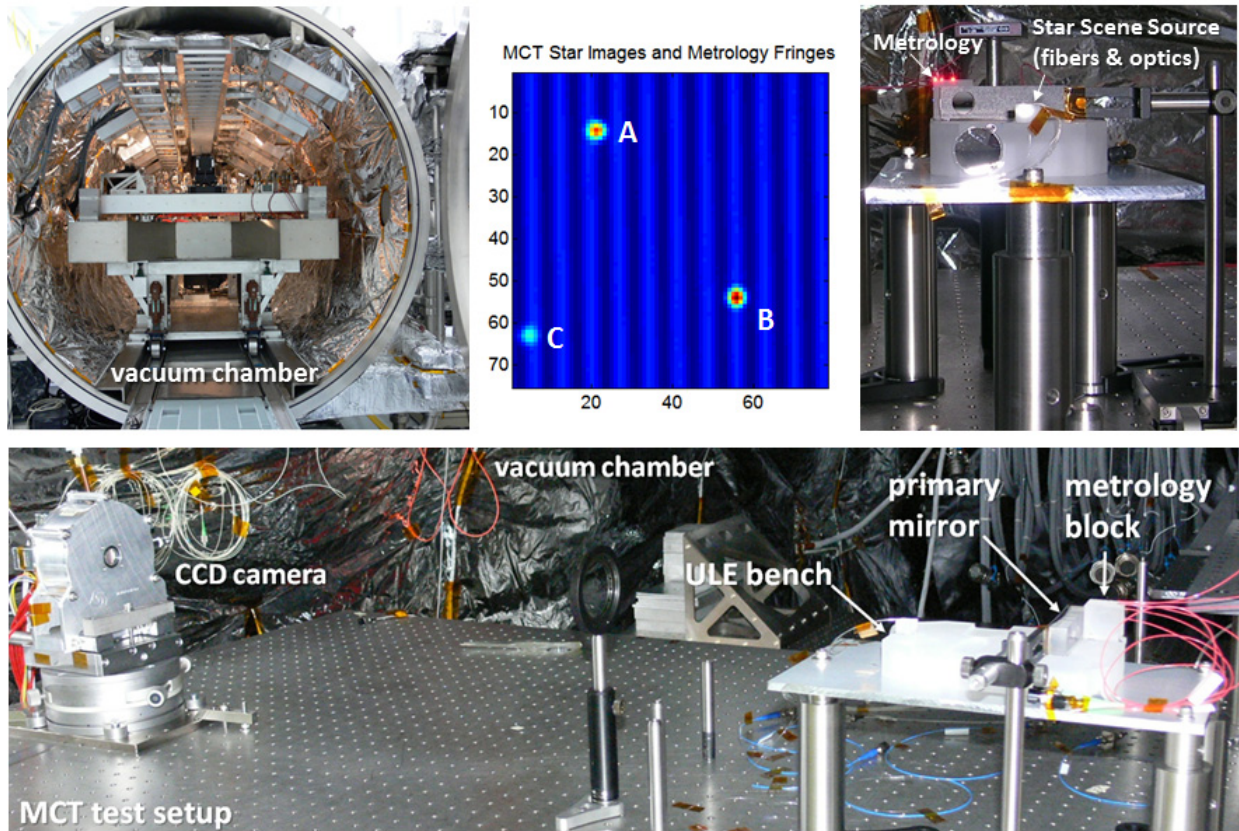


Figure 6: MCT test setup in the SIM vacuum chamber at JPL. Shown are the chamber (top left), the test setup (bottom), the ULE low-expansion optical bench (top right), and a single frame from the CCD with three stars and metrology fringes (top middle). In the bottom picture the test setup can be seen, with the camera on the left.

Figure 7 shows the metrology block and the imaging parabola during the installation phase. As highlighted by the circles in the picture, 3 horizontal and 3 vertical fibers were mounted on the block. The spacing between the fibers was designed to create a range of fringe spacings. On the right side of the figure can be seen 15 fringe patterns observed as each unique pair of fibers was turned on.

A more detailed look at the metrology system is offered by Figure 8. Acousto-optic Modulators (AOM’s) are used to switch on laser light to a pair of optical fibers, frequency shifting the light to one of the two fibers by a few Hz relative to the other. In general, an optical fiber projects laser light at divergent cone of about 10 degrees (deg) in diameter. On the CCD, the light from the two illuminated fibers interferes and, because of the frequency offset, the fringes “travel” across the CCD surface. The CCD in the experiment could be read at up to 50 frames per second (fps). If the applied (“heterodyne”) frequency offset is chosen at 5 Hz, then the output of any given pixel is a discretely sampled, 5 Hz sine wave with 10 samples per cycle (assuming 50 fps readout). If we compare two adjacent pixels we see two sine waves with a known phase shift. If the fringe spacing is, for example, 4 pixels, then adjacent pixels will have a $\lambda/4$ (i.e. 90 deg) phase shift. In other words, the measured phase difference between any two pixels is directly proportional to the distance between the pixels along the direction of the traveling fringe. By illuminating pairs of fibers with different relative positions, we can produce fringes traveling in different directions on the CCD surface and hence derive the relative

locations of all the pixels. This simplified scenario describes the essence of pixel metrology. The algorithm described in the previous section is actually used, to derive not just a pixel's location but the complete pixel response function.

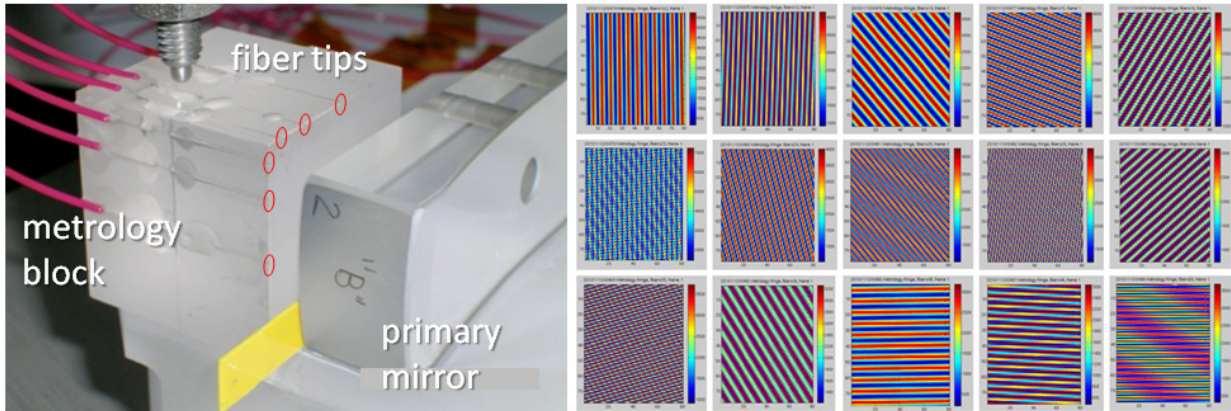


Figure 7: Close-up (left) of the metrology block and primary mirror in MCT, highlighting the metrology fiber tips, and (right) fringe patterns on the CCD for the 15 different lit fiber pairs.

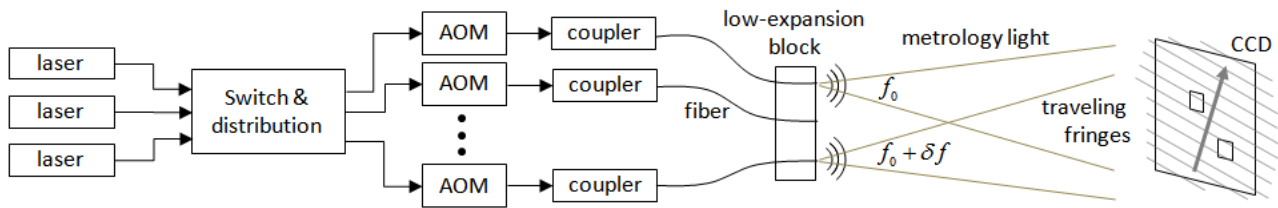


Figure 8: Heterodyne metrology uses lasers and AOM's to create beams that produce moving fringes on the CCD. The low expansion block and stable laser sources make the fringe spacing highly stable, creating a perfect yardstick that allows unprecedented performance in focal plane characterization.

4. INITIAL RESULTS

Before having to shut down the MCT effort late in 2010, we were able to conduct a number of tests on metrology and centroid estimation using real hardware. The left plot in Figure 9 displays the flat field response of each pixel using a single illuminated fiber. The variation is seen to be under 2%. The middle and right plots of Figure 9 display the measured effective pixel location deviations relative to a regular grid along x and y directions, respectively. We found that our CCD (an E2V CCD39) had a large step (a few percent of a pixel) between its left and right halves in one direction.

In a real astrometric application, the stellar image is spread over a number of pixels, and the averaging of the metrology over the pixels should offer some improvement. We tested this by averaging the metrology for a number of zones within the CCD, each 10x10 pixels in size. We then produced an Allan deviation plot, which shows the effect of increasing amounts of temporal averaging. In Figure 10, the left plot shows the mean behavior, for a number of these zones, versus increased integration time. In this test we reached 17 μ pix (400 pm in actual length units) after 25 seconds of averaging.

In MCT, we also used three white light fibers to simulate three stars (see top middle image, Figure 6), which we named stars A, B, and C. For star A and star B, the right plot in Figure 10 shows the Allan deviations of the centroids of each, as well as the Allan deviation of the difference of the centroids (i.e. the distance). It is the difference that is of interest in astrometry. In this experiment, where the centroids of star A or B moved together by about 250 μ pix on a time scale of 200 seconds, the separation of the two images averaged down to 30 μ pix after integrating for 200 seconds.

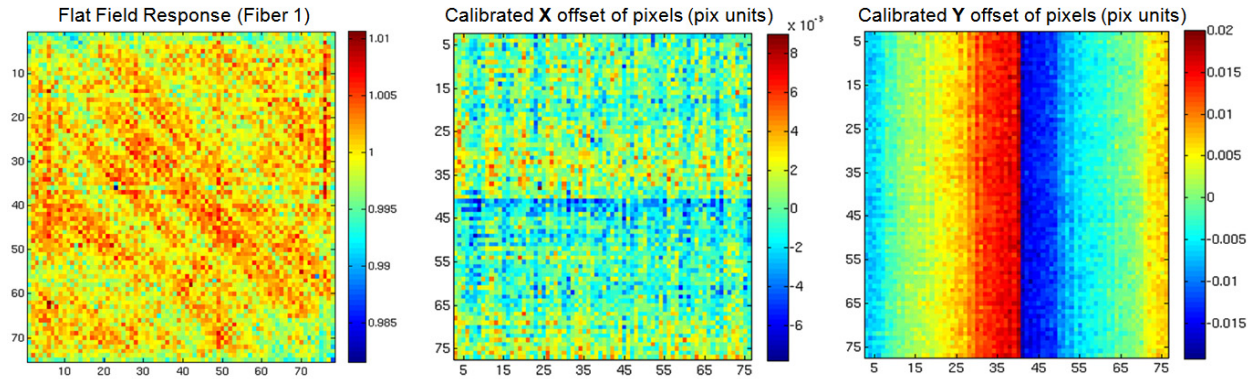


Figure 9: MCT test results showing the flat field response (left) and effective pixel location deviations from a regular grid along row (middle) and column (right) directions.

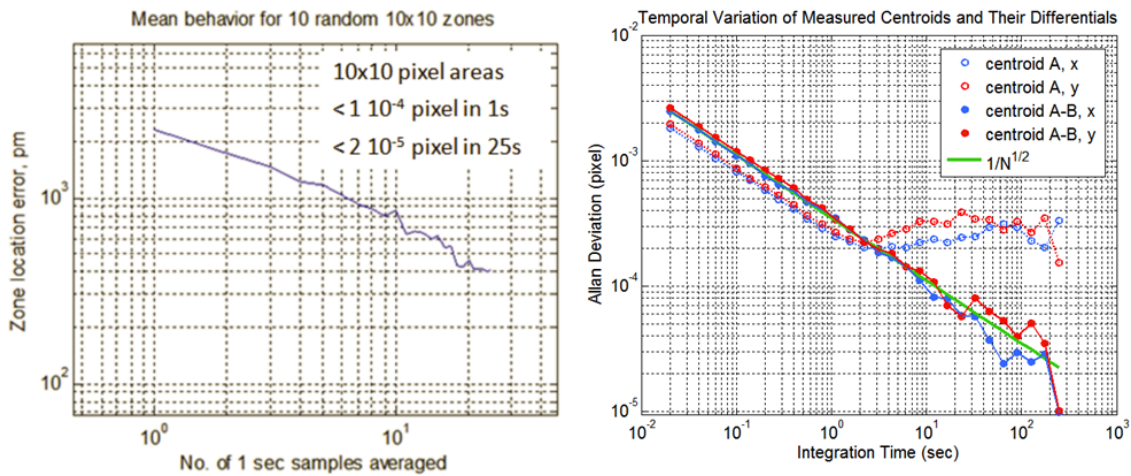


Figure 10: Metrology of pixel locations for a 10x10 zone achieves 20 μ pix accuracy in 25 sec (left). Also, the measured distance between the centroids of two artificial stars dips down to 30 μ pix after 200 seconds (right) under conditions where the individual centroids are moving by about 10X as much.

5. SUMMARY AND CONCLUSION

Micro-pixel centroiding holds promise as the enabling technology for low cost micro-arcsecond astrometry and particularly the search for Earth-mass planets in the habitable zones of nearby sun-like stars. We have developed an approach that uses precision metrology to calibrate the otherwise intractable focal plane systematic errors that would be encountered in getting down to micro-arcseconds in astrometric accuracy. We have checked the algorithmic aspects of our approach using simulations and begun testing the remaining aspects using a small testbed called MCT.

Using simulation we found that our image position sensing algorithm is capable of 4 μ pix accuracy in the presence of wavefront errors and displacements up to half a pixel. With the MCT testbed, we were able to calibrate the focal plane with a pixel-to-pixel differential measurement precision of less than 20 μ pix after 25 seconds of integration. Also, we demonstrated star-to-star differential measurement precision of less than 30 μ pix after 200 seconds of integration. The next set of tests will aim at systematic errors and aim to show accuracy at the few μ pix level by measuring the post-calibration inter-star distance repeatability under conditions where the actual distance is effectively constant.

ACKNOWLEDGEMENTS

This work was performed at the Jet Propulsion Laboratory, California Institute of Technology under contract with the National Aeronautics and Space Administration.

REFERENCES

- [1] Mayor, M. et al., "A Jupiter-mass companion to a solar-type star," *Nature* 378, 355 (1995)
- [2] Catanzarite, J. et al., "The Occurrence Rate of Earth Analog Planets Orbiting Sun-like Stars," *ApJ* 738 151 (2011)
- [3] Shao, M. et al., "NEAT: a Microarcsecond Astrometric Telescope," *Proc. SPIE* 8151 (2011)
- [4] Unwin, S. et al., "Taking the Measure of the Universe: Precision Astrometry with SIM PlanetQuest," *PASP*, Vol. 120, No. 863, p. 38 (2008)
- [5] Davidson, J., et al., "SIM Lite Astrometric Observatory," JPL 400-1360, 2/09, NASA/JPL (2009)
- [6] Shaklan, S. et al., "High-precision measurement of pixel positions in a charge-coupled device," *Appl. Opt.* 34, 6672-6681(1995).
- [7] Stone, R., et al., "A Comparison of Digital Centering Algorithms," *ApJ*, 97, 1227 (1989)
- [8] Kavaldjiev D., et al., "Subpixel Sensitivity Map for a Charge-coupled Device Sensor," *Optical Engineering*, 37, 948 (1998)
- [9] Zhai, et al., "Micro-pixel accuracy centroid displacement estimation and detector calibration," *Proc. R. Soc. A.*, doi: 10.1098/rspa.2011.0255 in print (2011)